Dynamic investigation of a concrete footbridge using finite element modelling and modal analysis

Fatemeh Hamid-Lakzaeian[a]* and Reto Cantieni[b]

[a]Faculty of Engineering, Department of Civil Engineering, University of Malaya, 50603 Kuala Lumpur, Malaysia

*Corresponding author: fati.lakzaian@gmail.com

[b]rci dynamics, Structural Dynamics Consultants, Raubbuehlstrasse 21B, CH 8600, Duebendorf, Switzerland

rci@rcidynamics.ch

Journal of Structure and Infrastructure Engineering

https://doi.org/10.1080/15732479.2011.611147

Abstract

In this article, the application of a manual updating method for finite element (FE) model updating of a concrete footbridge using modal analysis approach is described in detail. An FE model was developed using DIANA (FEM software package) to estimate the response of structure under free-vibration analysis. Afterwards, ambient vibration test (AVT) was conducted to extract the dynamic properties. The fundamental mode shapes of the structure were successfully identified applying ARTeMIS (modal analysis computer program). The mode shape pairs of initial FE model and a complete set of test results were employed for manual updating. A parametric study was carried out to specify the most sensitive parameters of the model. For this purpose, boundary conditions, mass density and Young's modulus of elasticity were examined as uncertain parameters. Attempts to calibrate the primary FE model revealed that the spring constants of supports were the most effective parameters for updating process. The FE model was calibrated considering three main criteria consisting of combination of natural frequencies/mode shapes and modal assurance criteria (MAC)/mode shapes. The calibration strategy performed in the present study, including parametric study on uncertain parameters of initial FE model, parameter and target response selection and MAC calculation based on modified formulation, has been discussed. The updated FE model and the measured mode shape counterparts exhibited very good correlation.

Keywords: footbridge; finite element modelling; ambient vibration testing; dynamic characteristics; model updating

1. Introduction

Applying finite element (FE) analysis method accompanied by experimental techniques has enabled the structural engineers to identify the structural properties accurately and provide reliable data to support calibration, updating and validation of numerical models used for design stages and structural health monitoring purposes. The system identification of civil engineering structures has been extensively discussed by Cantieni (2005) and Cunha and Caetano (2006). Dynamic assessment of bridges has been performed by Brownjohn et al. (2010), Reynders et al. (2010) and Caetano and Cunha (2004). Cantieni et al. (2008) and Turek et al. (2010) represented detailed description of FE model updating procedure of bridges. Pavic et al. (1998) introduced a calibration strategy using manual and automatic updating procedure and applied it on two footbridges. The calibration strategy performed in the present study consists of parametric study on uncertain parameters of initial FE model, parameter and target response selection, modal assurance criteria (MAC) calculation based on modified formulation and FE model updating comprising frequency/mode shape and MAC/mode shape criteria. The updated FE model and the measured mode shape counterparts exhibited very good correlation at the end of process.

2. Description of test structure

The test structure is a 37-m reinforced concrete footbridge in the university campus, dating back to the 1950s and composed of three spans fixed differently at two end abutments; one abutment being stuck in the mud and the other being cut from the pavement. There are four structural parts that connect the footbridge to the ground; two cross-beams at end abutments and two cross-frames at intermediate supports. Also, there is a longitudinal I-beam stiffener at mid-span, underneath which the height of its web varies along the longitudinal axis of the element. The depth of the concrete slab is 0.09 m, with a curve shape in elevation view of structure (Figure 1). The components labelled as Det 1, Det 2 and Det 3 denote cross-beam, cross-frame and I-beam stiffener, respectively. Further details about the cross-section, plan and elevation views are given in Figure 2.

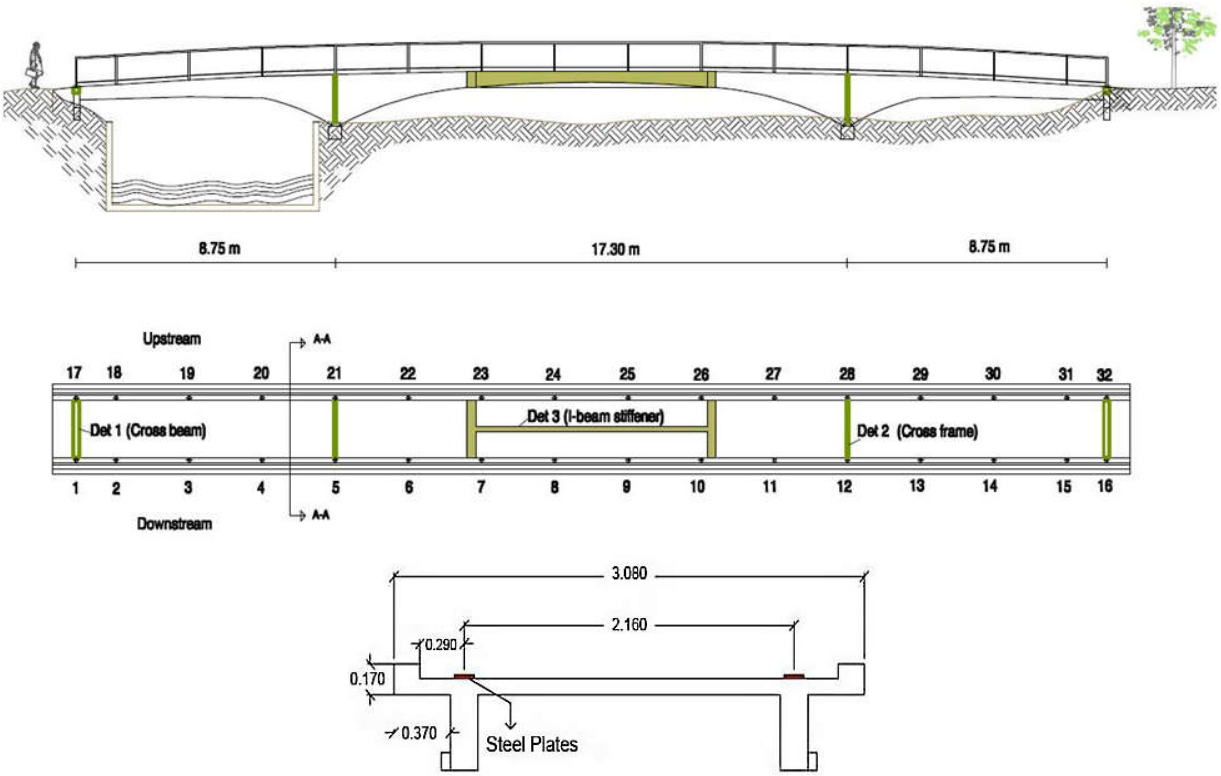

Figure 1. Elevation-longitudinal section, plan and cross-section (section AA) views of footbridge.

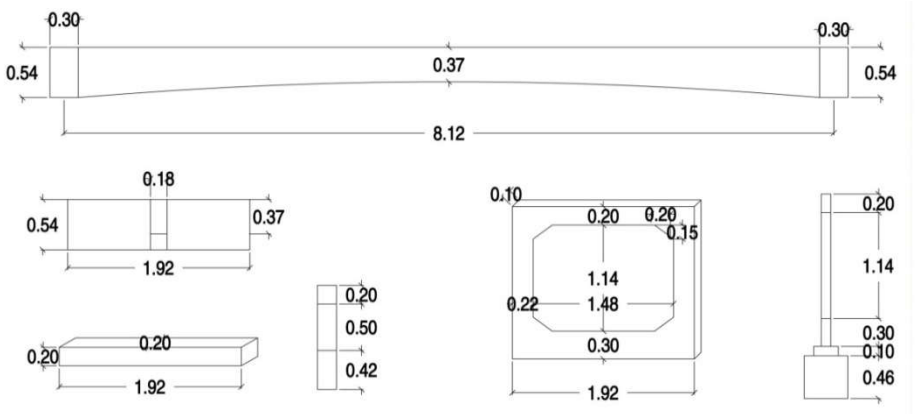

Figure 2. Det 1: End abutment cross-beam at left bottom, Det 2: Intermediate support cross-frame at right bottom, Det 3: Longitudinal I-beam stiffener in mid-span (longitudinal section on top, cross-section on top left).

3. Finite element modelling

An FE model of the footbridge under investigation was developed using DIANA 9.3 (DIANA 2009). Two types of elements were used to build the FE model of the structure. As the thickness of the footbridge deck is small in relation to the width of the structure, a three-dimensional (3D) curve shell element was used to model the deck. The same element type was used to create the side walls. To model the other components comprising cross-frames at intermediate supports, cross-

beams at end abutments and I-beam stiffener at mid-span, a 3D beam element was employed. QU8 CQ40S is a quadrilateral, iso-parametric curved shell element. Five degrees of freedom (DOF) have been defined in every element node, including three translations and two rotations. The basic variables in the nodes of the curved shell elements are translations u_x, u_y and u_z in the global XYZ directions and the rotations j_x and j_y, respectively, around the tangent plane. Curve shell elements may be loaded with a concentrated load or with a distributed load on one or more edges or over the entire element face. The thickness of shell elements may be uniform or non-uniform. BE3 CL18B, a curved three-node, 3D class-III beam element, was employed to model cross-frames, I-beam stiffener and cross-beams. The basic variables of beam element classified as class III are the displacements in the nodes: six translations u_x, u_y and u_z and six rotations j_x, j_y and j_z. Beam elements may be loaded with a concentrated load or with a live load distributed along the beam axis. The element is numerically integrated along the beam axis; therefore, the dimensions of the cross-section may vary along the beam axis (DIANA 2009). For three sets (flanges of I-beam, cross-beam and cross-frame) with perpendicular direction to the longitudinal axis of the structure, three external–local axes were defined, as it was required for a 3D beam element. The footbridge was modelled as reinforced concrete with Young's modulus of elasticity of 18.3 KN/mm^2, Poisson's ratio of 0.2 and mass density of 2545 Kg/m^3.

Definition of boundary conditions for the footbridge in question was a decisive subject due to specific condition of abutments which one was being stuck in the mud and the other one being cut from the pavement and totally free. The FE model at four points which cross-beams link two side walls of the structure (two pairs of P28-P48 and P38-P58), and at one of abutments embedded in the mud (P139-P159) was equipped with 3D elastic supports (Figure 3). The stiffness values for springs in X and Y directions were specified as 1E + 8 N/m, and in Z direction, as 1E + 7 N/m. At the other side, where cross-beam (P28-P48) exists, the edge of the footbridge (P129-P149) does not have any connection with the ground; hence, it was assumed as free, and no spring was defined for this end. Fixed support was applied to introduce four connection points of structure at mid-span (P2, P3, P4 and P5), since they looked like to be set firmly in the ground. The mass modelling adopted is lumped mass modelling. A free-vibration analysis was performed to extract eigenvalues (frequencies) and eigenvectors (mode shapes) of the footbridge. Information based on preliminary FE model provided a proper image of the expected eigenvalues and eigenvectors of the structure (Figure 4). The range of natural frequencies was estimated from 6.02 Hz (lateral mode) to 19.61 Hz (second torsion mode), though it needs to be verified and validated by modal testing.

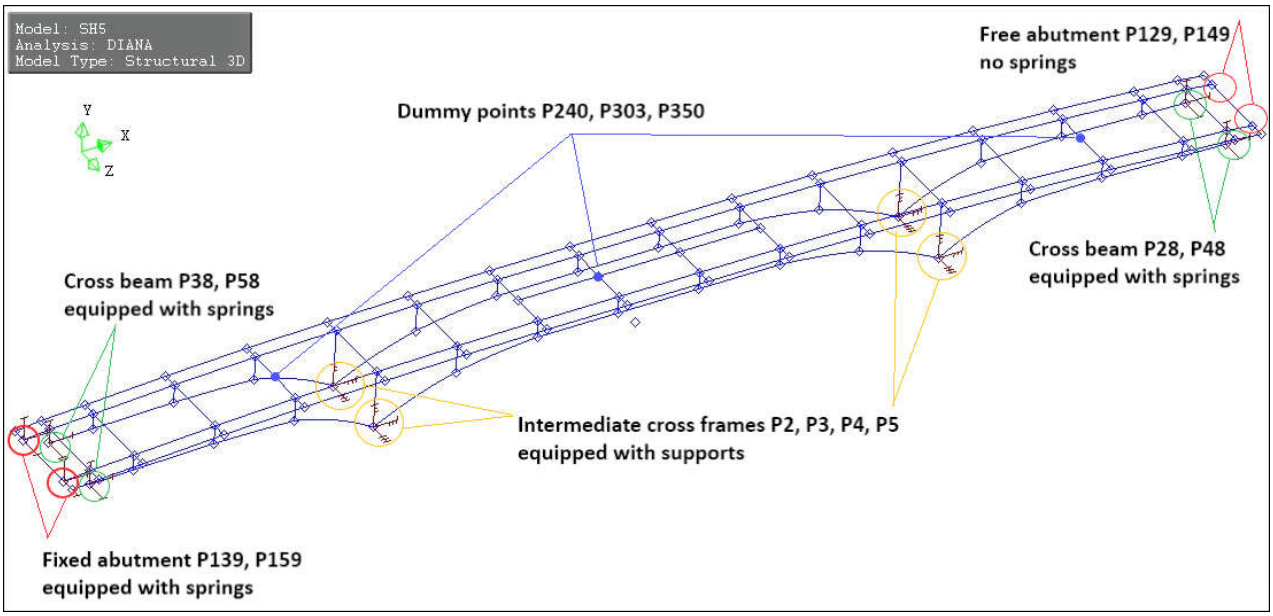

Figure 3. Perspective display of test points based on results of FE model.

 FE mode 1 (lateral) at 6.02 Hz	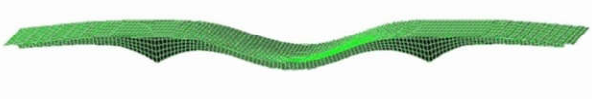 FE mode 2 (1st vertical) at 8.29 Hz
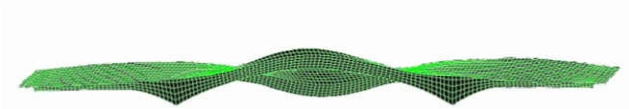 FE mode 3 (1st torsion) at 10.82 Hz	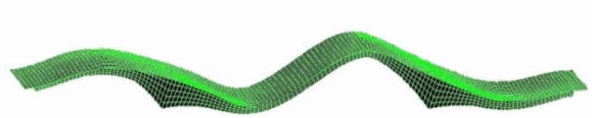 FE mode 4 (2nd vertical) at 11.92 Hz
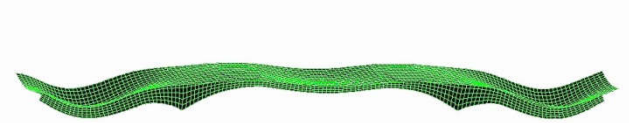 FE mode 5 (3rd vertical) at 17.82 Hz	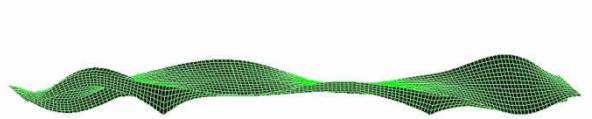 FE mode 6 (2nd torsion) at 19.61 Hz

Figure 4. First six modes of vibration calculated from the initial FE model.

4. Ambient vibration testing

The mode shapes extracted from initial FE model were employed as a guide to plan the test layout, the location of reference sensors and the movement of rovers for ambient vibration test (AVT). The availability of using seven sensors for the test provided the opportunity to arrange the

test strategy using more than one reference channel. The perspective view of footbridge including marked test points is given in Figure 3. The solid points marked on the surface of structure were all test points, except two pairs (P129-P149 and P139-P159). The three points marked as P240, P303 and P350 at centre line of the structure were adopted as dummy points to complete the number of sensors in some setups of test layout. To identify the footbridge, two sets of AVT were conducted. The first test measured the structure in one dimension using three vertical 1D reference points (TP9, TP19 and TP29) at downstream and upstream sides, whereas for the second test, 2D measurement was applied using one 3D reference at TP26 (Figure 1). The abbreviated phrase TP stands for test points in two test layouts.

In the first AVT (1D measurement), the number of three references was employed, and the other four rovers were distributed in eight setups to measure responses at three spans per setup. OROS 36, which is a multi-analyzer/recorder with 32 channels and resolution of 24 bit, was employed to acquire the test data. The adopted data acquisition parameters were set at 500 s and 200 Hz for time window length per setup and sampling frequency, respectively. The measurement data were analyzed using ARTeMIS (ARTeMIS 1999–2002), and five modes of vibration were identified. AVT was repeated to measure the footbridge vertically and longitudinally/laterally with sixteen setups applying a 3D reference sensor at TP26, whereas four rovers scanned the structure in two dimensions. Figure 5 illustrates the geometry of setups 6 and 12 of first (up) and second (down) tests, respectively.

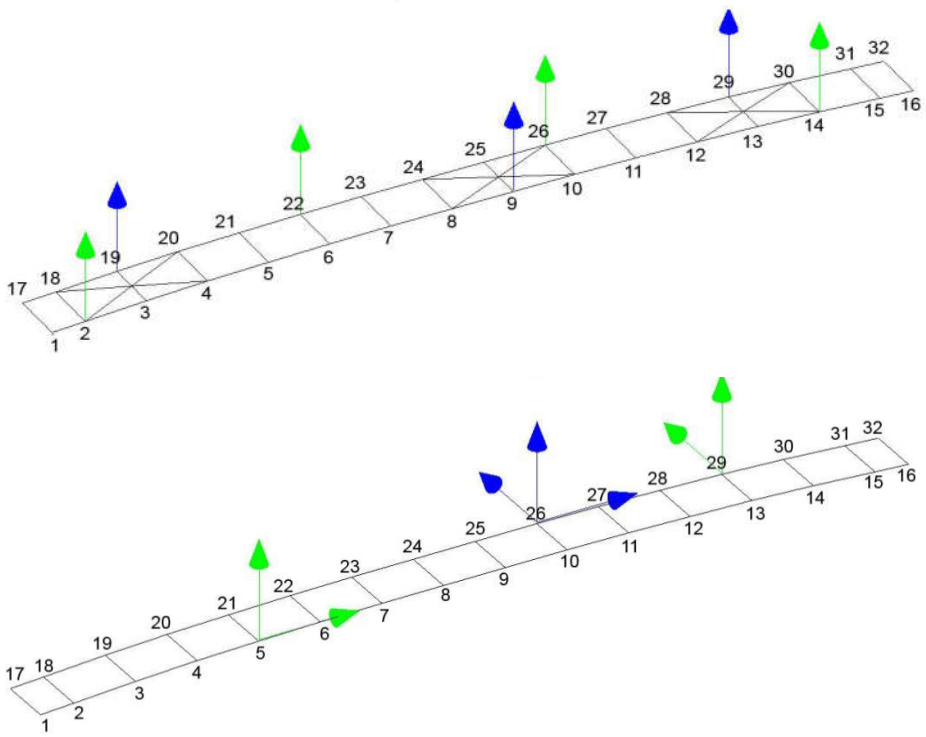

Figure 5. Geometry of setup six of first AVT (top), and setup 12 of second AVT (bottom). Note: Blue: reference points, green: rovers.

Analysing the data obtained verified the results of first AVT as well as revealed a lateral mode shape at 4.27 Hz. The singular value decomposition (SVD) diagrams of two ambient measurements are shown in Figure 6. Although different input sensitivities applied for second AVT (0.5g for horizontal and 2.5g for vertical sensors), but due to higher quality of mode shapes obtained from first test compared to their counterparts from second one, the number of five mode shapes were selected from first AVT and the lateral mode of second test was added to the set of test data. Therefore, a complete set of two measurements consisting of six mode shapes, as shown in Figure 7, was employed for model updating.

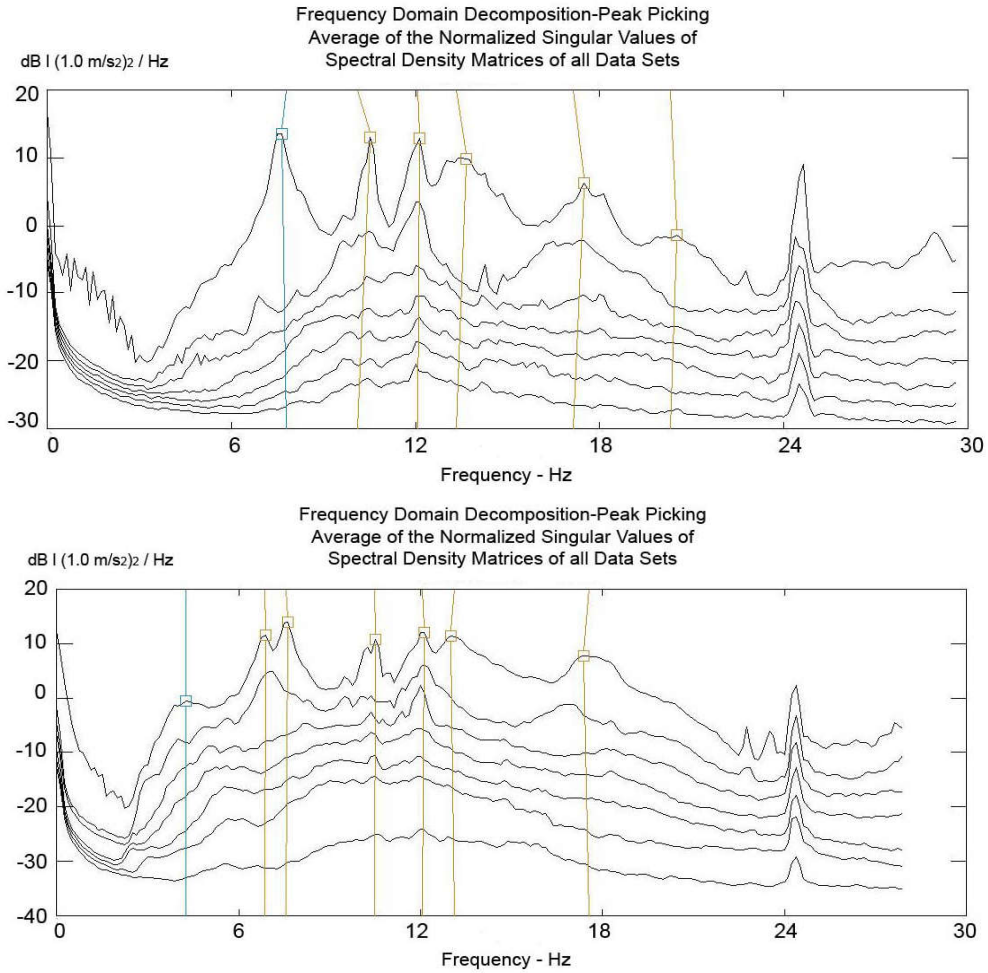

Figure 6. EFDD SVD diagram of first and second vibration tests.

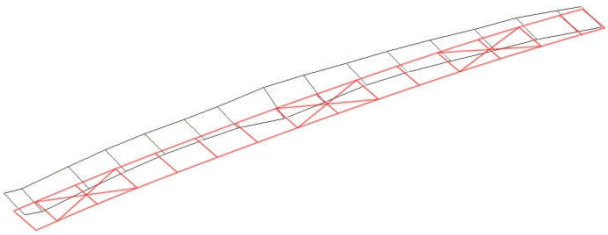

EFDD lateral mode at 4.27 HZ

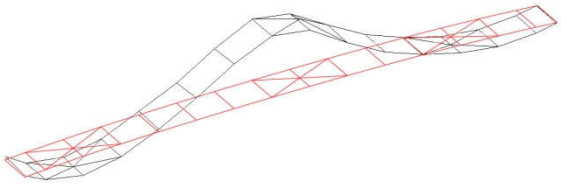

EFDD 1st vertical mode at 7.56 Hz

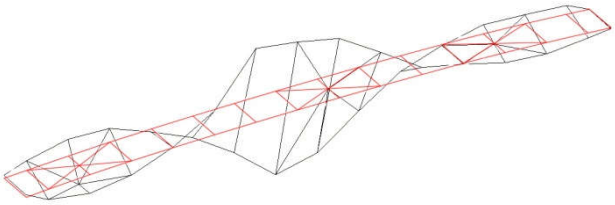

EFDD 1st torsion mode at 10.52 Hz

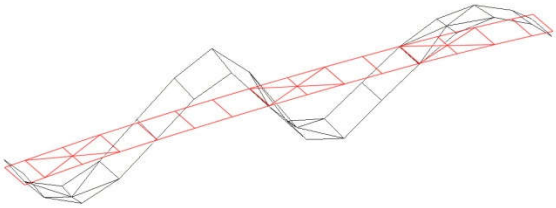

EFDD 2nd vertical mode at 13.38 Hz

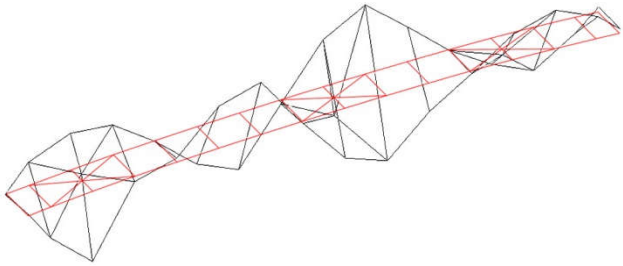

EFDD 2nd torsion mode at 17.63 Hz

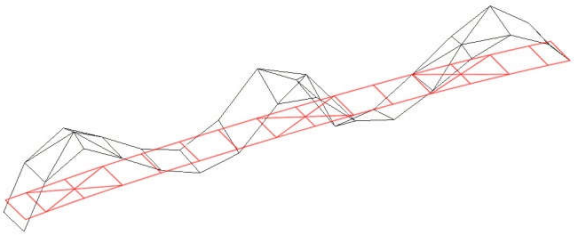

EFDD 3rd vertical mode at 20.33 Hz

Figure 7. Vibration mode shapes identified by first and second AVT.

5. FE model tuning

The strategy implemented for tuning and updating of FE model composed of (1) parametric variation, (2) parameter and target response selection, (3) MAC calculation and (4) frequency/mode shape and MAC/mode shape criteria application, which is represented as a flowchart in Figure 8.

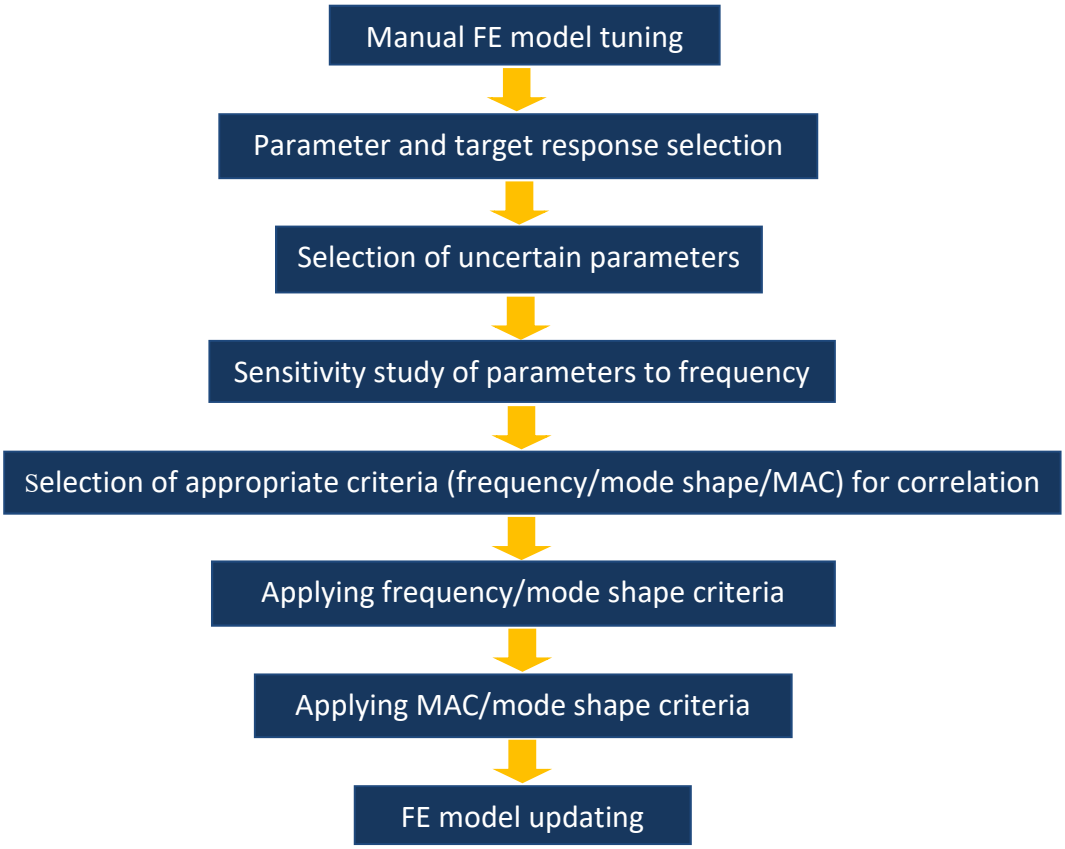

Figure 8. Flowchart of FE model updating.

5.1. Parameter variation

Visual comparison between measured and analytical mode shape pairs revealed that the flexible supports were required to be introduced for intermediate supports, same as end abutments. There were three justifications for such modification. The first was the existence of third bending mode with too much lower amplitude at the mid-span, whereas the test counterpart showed larger amplitude at the same place. Also, the torsional mode shape which appeared after first one did exhibit asymmetric behaviour at two end abutments, and the shape of the mode was dissimilar to the relative test pair. In addition, based on test results, intermediate supports showed some movements, whereas in initial FE model, they were considered fixed. Therefore, spring supports were introduced for mid-span supports.

Properties that affect the system's modal behaviour mainly are geometry, material properties as well as boundary conditions. To calibrate the FE model, sensitive parameters with uncertainties are required to be reasonably verified. Following modification on intermediate cross-frames, a parametric study was performed on uncertain parameters of the FE model, which were Young's

modulus of elasticity (E), mass density (r) and stiffness values of spring supports. Ten iterations with different mass densities and E revealed that the effect of the two mentioned parameters on FE model was not significant (Figures 9 and 10). As the graphs show, there was a rather constant trend between FE-test mode shape counterparts while the E and mass density vary. However, the graph trend for all modes was slightly rising for E and falling for r, but that was not much sizable. As a result, the two aforementioned parameters were not considered the most sensitive parameters for model updating calculations. Another issue was concluded from Figures 9 and 10 that there were large differences between calculated and measured frequencies for all mode shape pairs except lateral mode.

In order to determine the appropriate range for stiffness values of footbridge supports and proceed to parameter selection step, the ratio of analytical frequency to measured frequency for all six modes was calculated (Figure 11). The values selected for spring constants were in the range from 1E + 7 to 1E + 10 N/m for all supports. As it can be seen from Figure 11, the respective lines for five mode shapes cross the horizontal line, except T2 (second torsional mode shape measured at 17.63 Hz), whereas the cross points were in a quite large range of spring constants.

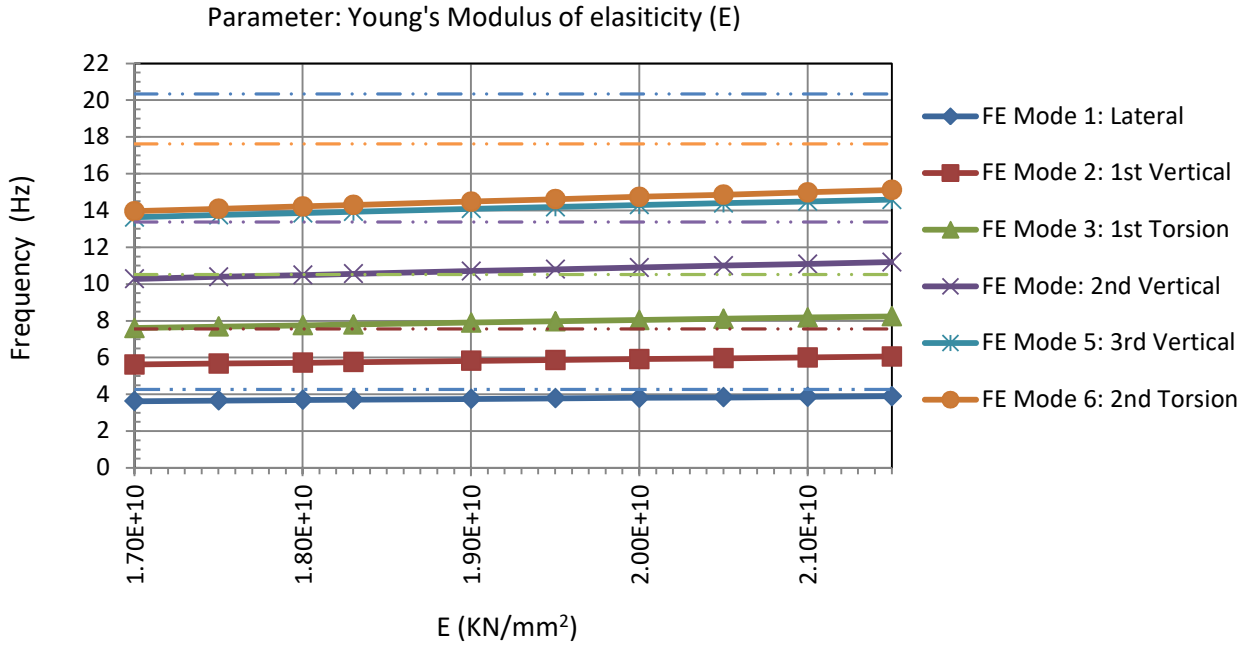

Figure 9. Parameter variation (E); FE: solid lines; measured: dashed lines

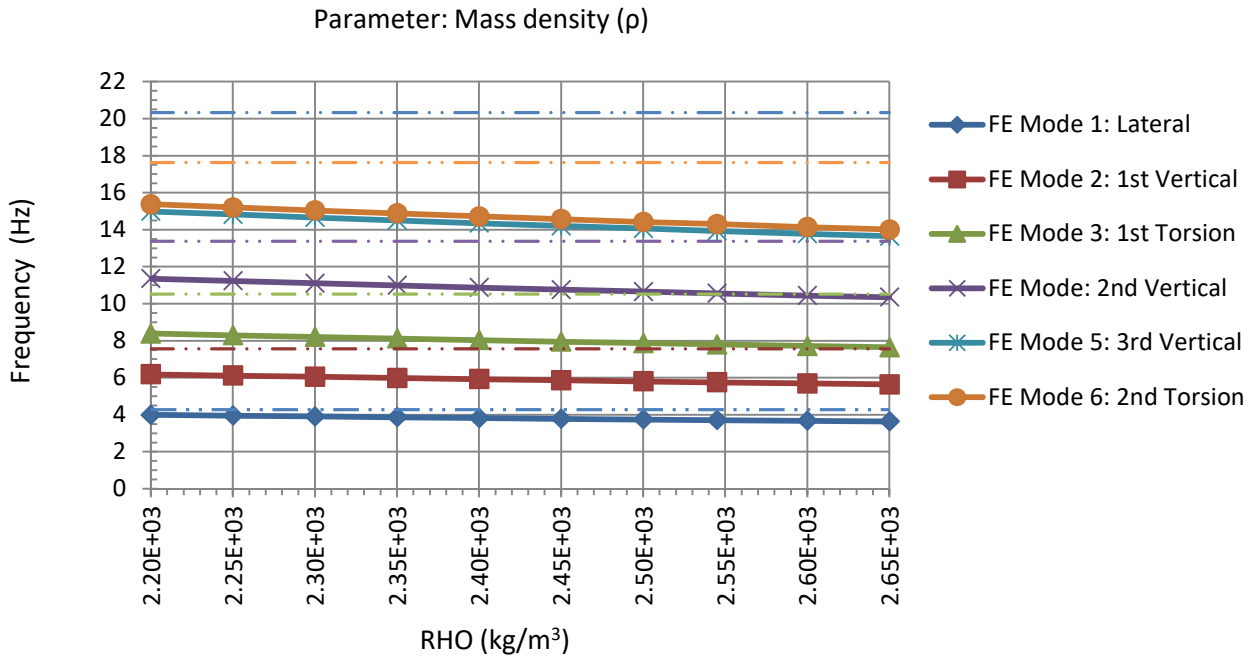

Figure 10. Parameter variation (ρ); FE: solid lines; measured: dashed lines.

5.2. Parameter and target response selection

Concerning the selection of parameters for model updating, the most important parameters for this case study were spring constants, as discussed in previous section. There were two issues that made a considerable uncertainty about boundary conditions of the structure. First was the settlement of the footbridge at one side, and the second was the particular condition of the soil. The soil surrounding the structure was not rigid enough and made an unknown behaviour for all the supports. Basically, boundary conditions are important, since the support conditions are the most significant parameters influencing the static and dynamic behaviours of a civil engineering structure, and for this specific case study, the behaviour of supports was not known as the structure was surrounded by mud. Therefore, the boundary conditions (spring constants) were selected as updating parameters. The supports were grouped at four sets which represented the boundary conditions at cross-beam at free abutment side, intermediate supports, cross-beam at fixed abutment side and fixed abutment itself.

The three different criteria selected as responses in updating procedure were resonance frequencies, MAC and mode shapes. For model updating of the footbridge under discussion, all three criteria were considered in calculation. The procedure was two-fold: First, calculating

frequencies for all six mode shape pairs for each group of supports versus measured frequencies, and second, calculating MAC values for the same range of spring constants.

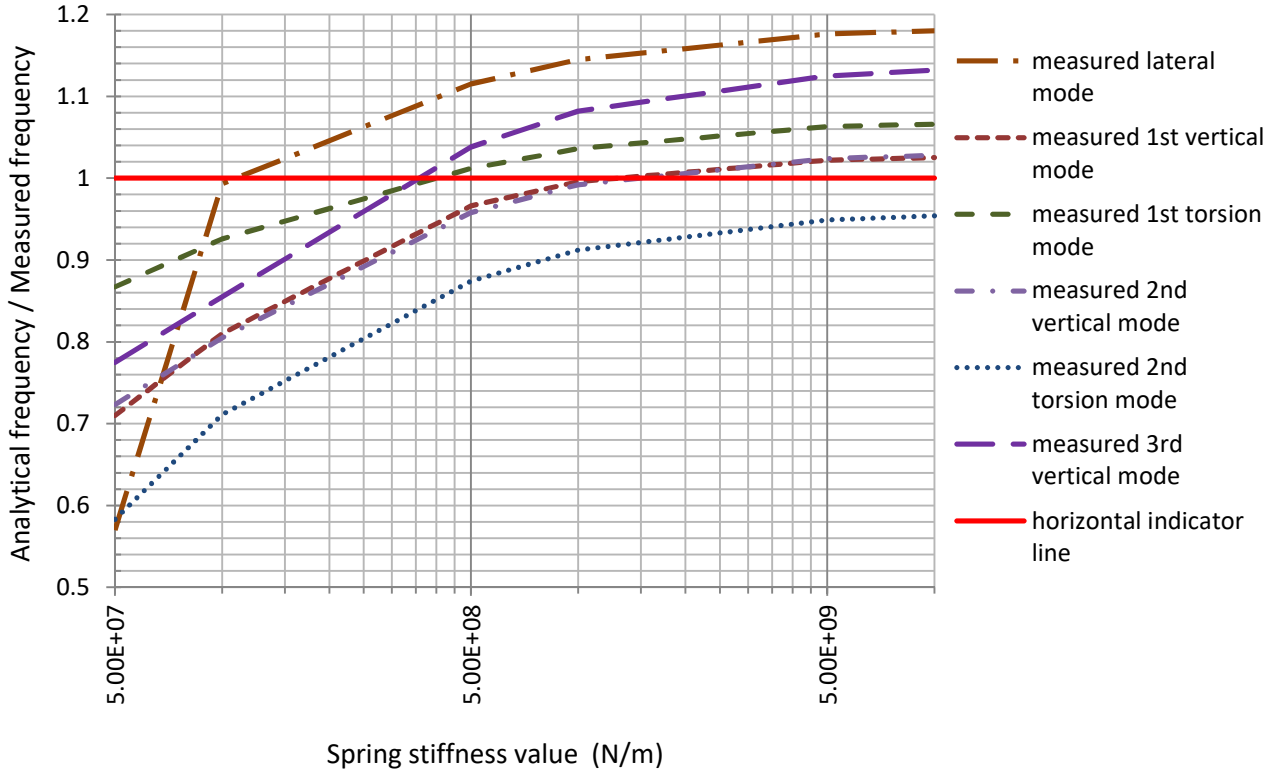

Figure 11. Choice of appropriate stiffness for spring supports (K_x, K_y, K_z for all supports).

5.3. MAC calculation

To validate the theoretical model, several steps should be taken. The first step is to make a direct and objective comparison of specific dynamic properties between analytical and experimental models. The second is to quantify the extent of the differences among FE-test data. Finally, the third step is to make modifications on FE-test sets of data to reduce the difference (Ewins 1997). There are many different correlation techniques to compare analytical and experimental modal vectors. The correlation techniques can be classified into techniques relating to the modal correlation in a vector sense and those relating to the correlation in a DOF sense; both of these classes can be further broken down into those techniques which do not employ any mass scaling and those techniques that apply mass scaling. In general, the techniques of first group are easier to implement. Techniques that apply mass scaling are more difficult to use since the mass matrix needs to be condensed, but usually offer more robust evaluation of the data evaluated. MAC as a vector-based technique is extremely useful, which gives a first indication as to the level of

correlation that exists between the analytical and experimental modal vectors. MAC is ideal to identify which analytical modes correspond to which experimental modes and is very helpful when identifying mode switching. That is, very sensitive to the DOF that are largest in value and is very insensitive to very small DOF in the mode shape vector. Mass weighting is not employed in this formulation, and consecutively, mass reduction is not needed, but the scaling effects of the mass matrix are useful in weighting various DOF for a correlation study. The vector correlation techniques evaluate the vector in a global sense, and the correlation of the vector is stated in terms of a scalar quantity that provides a measure of the level of correlation achieved (Avitabile 1998).

While MAC is a simple matter to compare the natural frequency characteristics, it is generally more challenging to obtain a quantitative comparison of the mode shapes. MAC is the technique employed to quantify the differences between the two mode shapes and devised to provide a single numerical value that indicates the correlation between mode shapes. It was introduced by Allemang (1982, 2003). The most common formulation of MAC used for comparing experimental and analytical models was defined by Maia and Silva (1997) as Equation (1):

$$\mathrm{MAC}\ (\{\Phi_x\}_i,\{\Phi_A\}_j)=\frac{\left|\{\Phi_x\}_i^T\{\Phi^*_A\}_j\right|^2}{(\{\Phi_x\}_i^T,\{\Phi^*_x\}_i)(\{\Phi_A\}_j^T,\{\Phi^*_A\}_j)}$$

Equation (1)

where Φx and Φ_A are eigenvector sets and denote mode shapes of experimental and analytical results. Equation (2) is a modified form of Equation (1) and was defined for the purpose of MAC calculation. The formula was applied to obtain a quantitative comparison of the FE-test mode shapes calculated for n nodes of structure:

$$\mathrm{MAC}\ (i)=\frac{(\sum_{j=1}^{n}(U_{ai})_j\ \times (U_{ei})_j)^2}{\sum_{j=1}^{n}\left((U_{ai})_j\ \times (U_{ai})_j\right)\times\ \sum_{j=1}^{n}((U_{ei})j\ \times (U_{ei})_j)}$$

Equation (2)

where U_{ai} and U_{ei} stand for vertical translational displacements of eigenvectors of FE (analytical) and test (experimental) models. The index i denotes the number of each mode shape pair. MAC

was calculated by a modified 1D MAC formulation that utilised DIANA and ARTeMIS output files to compute the level of correlation among FE-test mode pairs.

6. Manual FE model updating

The three criteria of FE model updating, i.e. natural frequency, mode shape and MAC, were considered as described in section 5.2. To update the FE model of the case study, dual combinations of frequency/mode shape and MAC/mode shape were taken into account.

6.1. Frequency/mode shape criteria

Based on the results obtained in parameter and target response selection and the appropriate range for spring constants, natural frequency and mode shape pair correlations were calculated. Two supports at cross-beams of free and fixed abutment sides, fixed-end abutment itself and one intermediate support were selected at opposite sides (P48, P38, P159 and P2). Meanwhile, an extra set of calculation was performed for support at P5, which demonstrates other intermediate support at opposite side. The set was calculated to investigate whether there was any considerable change between spring supports at two sides of the structure. The results revealed that there was not much difference between the spring constants at downstream and upstream. More investigation was conducted to find out the best range for stiffness values of each support. As two examples, the following six graphs (Figures 12–17) concerning frequency changes for P2 as an intermediate support and P38 as cross-beam at end abutment have been represented. Apparently, there was a quite similar trend for all spring supports in the three directions, although based on optimisation study of spring constants, different starting and ending values for each support were considered in order to produce the least frequency difference between FE and test models. Modification on stiffness values resulted in good agreement between all mode shape counterparts. The higher values for stiffness were also examined, but for the following reasons, they were not considered to be presented in the graphs: the difference between FE-test frequencies increased largely for lateral and second torsional modes, and also, lower MAC values were produced for V1, T1, V2 and V3. Consequently, based on the results of overall improvement on FE-test frequency differences and MAC values for all sets of supports, the final results of MAC are presented in section 6.2.

6.2. MAC/mode shape criteria

MAC was calculated for all nine groups of spring supports (Figure 18). The arranged sets of supports were the same sets as used for calculation of previous section. The modified MAC formulation did quantify the differences between two sets of FE and vibration test models. Vertical direction was considered for MAC calculation. As it could be expected, there was low MAC value (<60%) for lateral mode shape of groups 1–5. The possible reasoning was the modified formula calculates the MAC value in vertical direction only, whereas that mode shape was a lateral one. Also, there was low agreement for a few groups of two mode shapes: for T2, the value of 63%, and for V3, the values of 56%, 66% and 64%. The aforementioned stiffness sets contained values from 7.9E + 6 to 27E + 6 N/m for K_z at location of P4 and from 4.9E + 7 to 18E + 7 N/m for K_x at location of P3. The starting values for these two ranges were the lowest among other starting values of K_x and K_z. As the graph illustrates, there were very good correlations for the three modes of V1, T1 and V2. Such prediction was possible due to the results of previous section for these three mode shapes, as close relation did exist between analytical and measured frequencies of those modes.

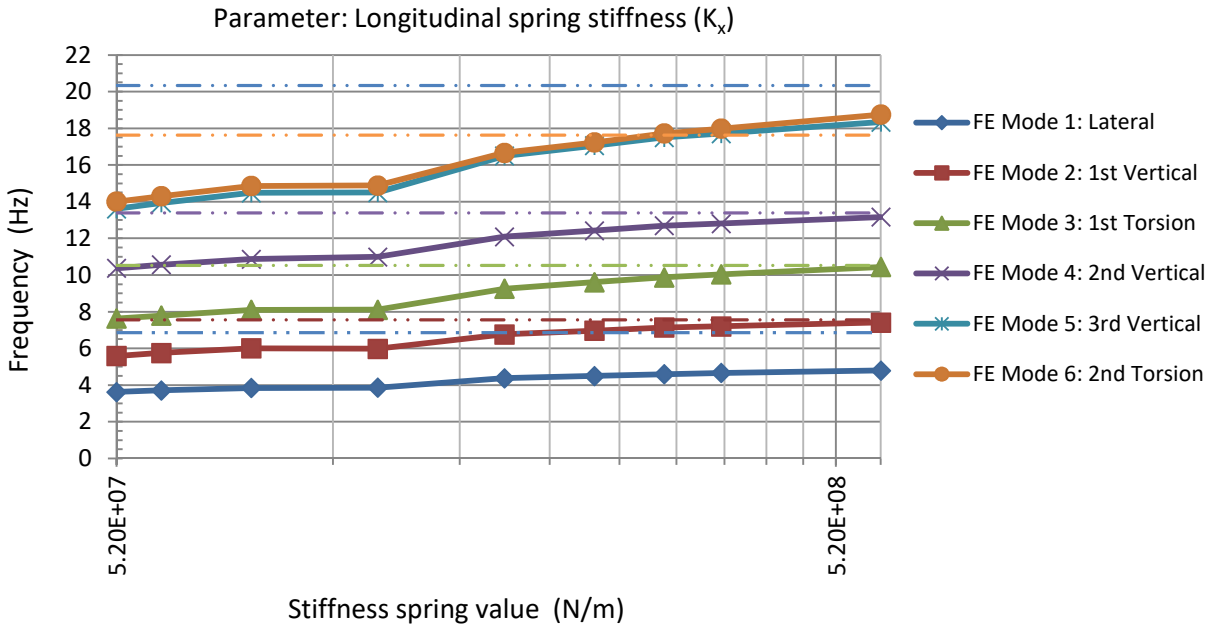

Figure 12. Parameter variation K_x (P2 as intermediate support); FE: solid lines; measured: dashed lines.

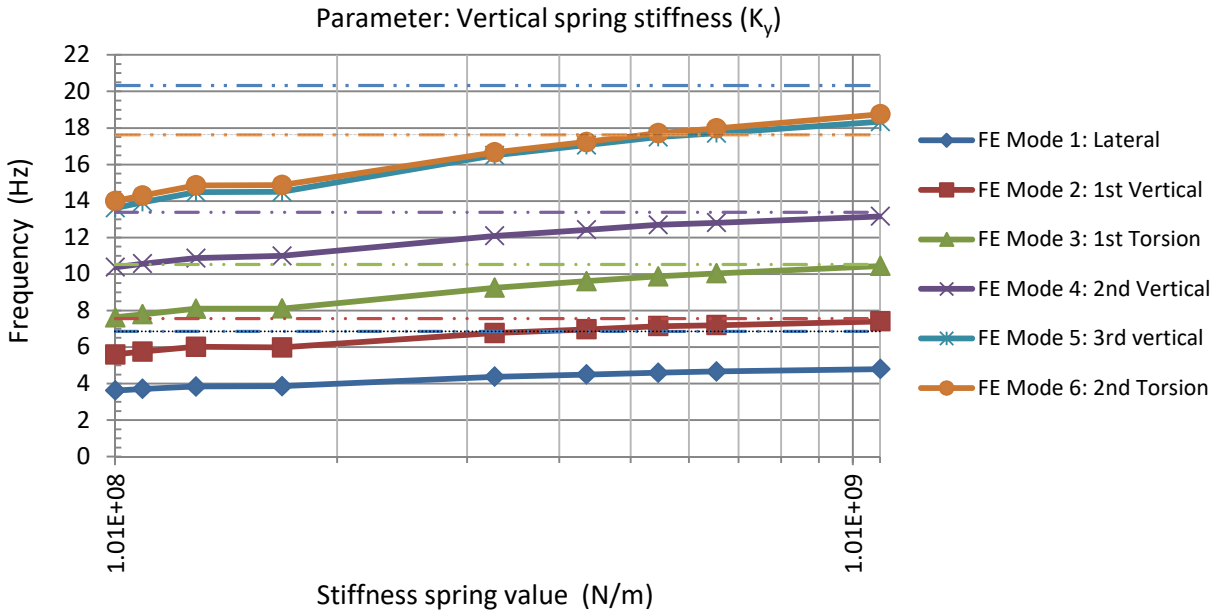

Figure 13. Parameter variation K_y (P2 as intermediate support); FE: solid lines; measured: dashed lines.

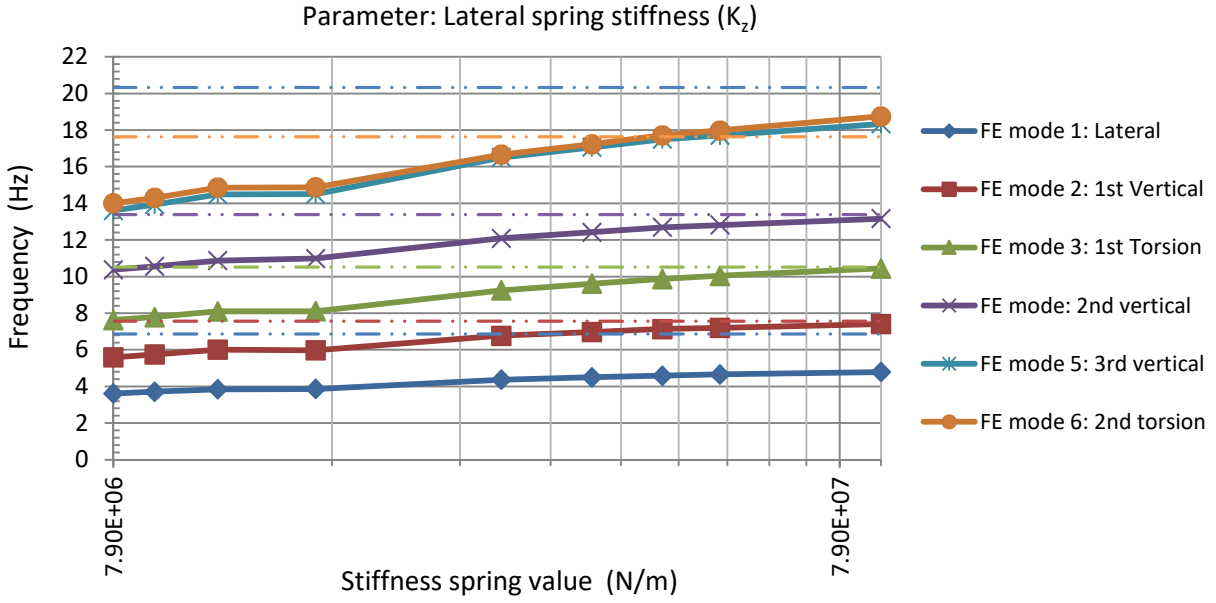

Figure 14. Parameter variation K_z (P2 as intermediate support); FE: solid lines; measured: dashed lines.

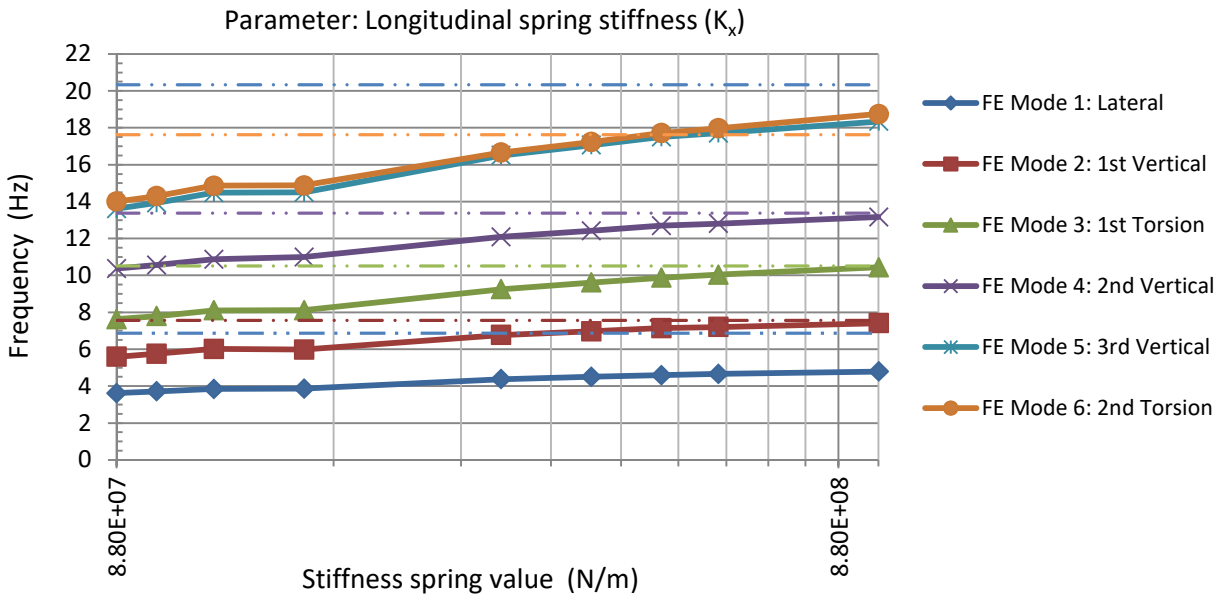

Figure 15. Parameter variation K_x (P38 as cross-beam at fixed abutment); FE: solid lines; measured: dashed lines

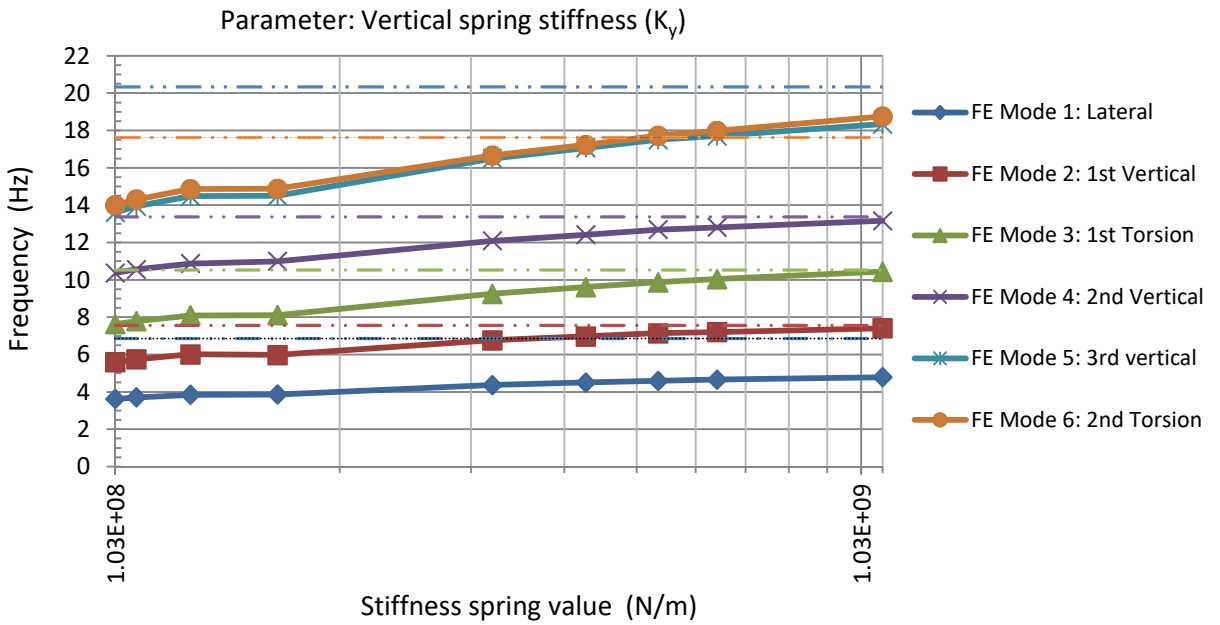

Figure 16. Parameter variation K_y (P38 as cross-beam at fixed abutment), FE: solid lines; measured: dashed lines.

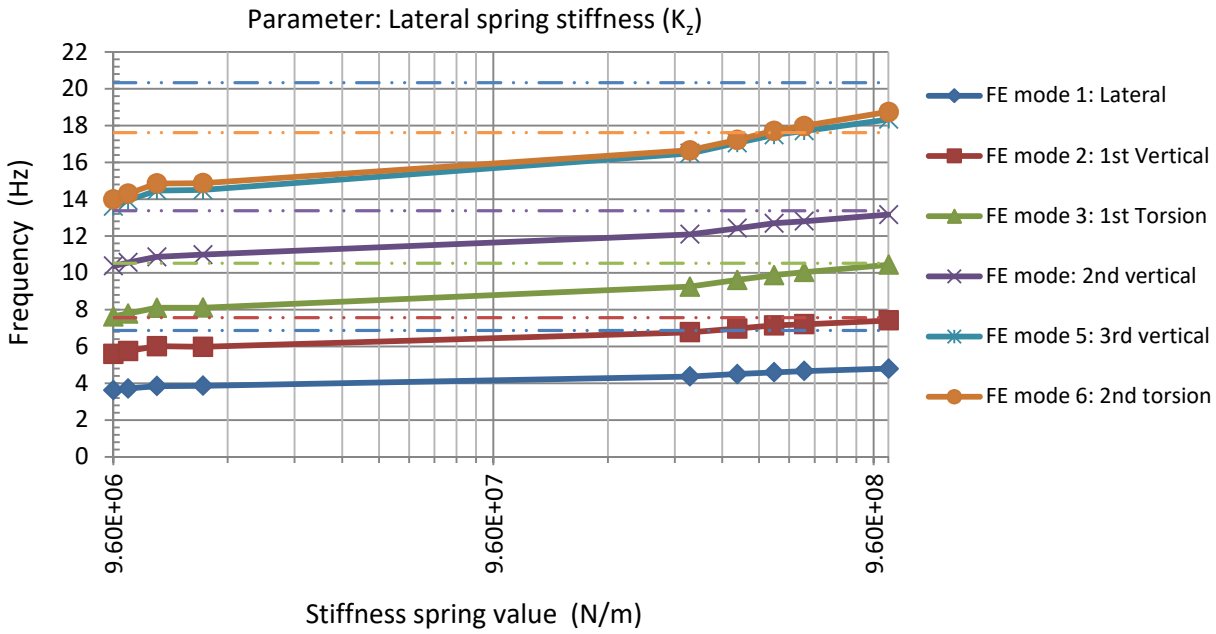

Figure 17. Parameter variation Kz (P38 as cross-beam at fixed abutment); FE: solid lines; measured: dashed lines.

6.3. FE model updating

The results obtained from FE model tuning were used for the final step of FEM updating. In order to select the best values for spring constants to get higher agreement between FE-test mode shape pairs, the boundaries as follows were set for spring stiffness: K_x: 2.4E + 8 to 1.05E + 9 N/m, K_y: 4E + 8 to 1.15E + 9 N/m and K_z: 3.6E + 7 to 1.05E + 9 N/m. To get finer results, it was required that two main criteria were considered: frequency and MAC. It is essential to mention that the information of mode shapes as the other main criteria for updating has been already included in MAC and frequency calculations. Comparing the results of frequency pairs and MAC values in selected range resulted in the information given in Table 1: The columns IV and V represented starting and updated values of parameters in manual model updating procedure. The values listed included whole values used for FE model tuning (frequency/mode shape and MAC/mode shape calculations), which consist of above selected range for K values in three directions.

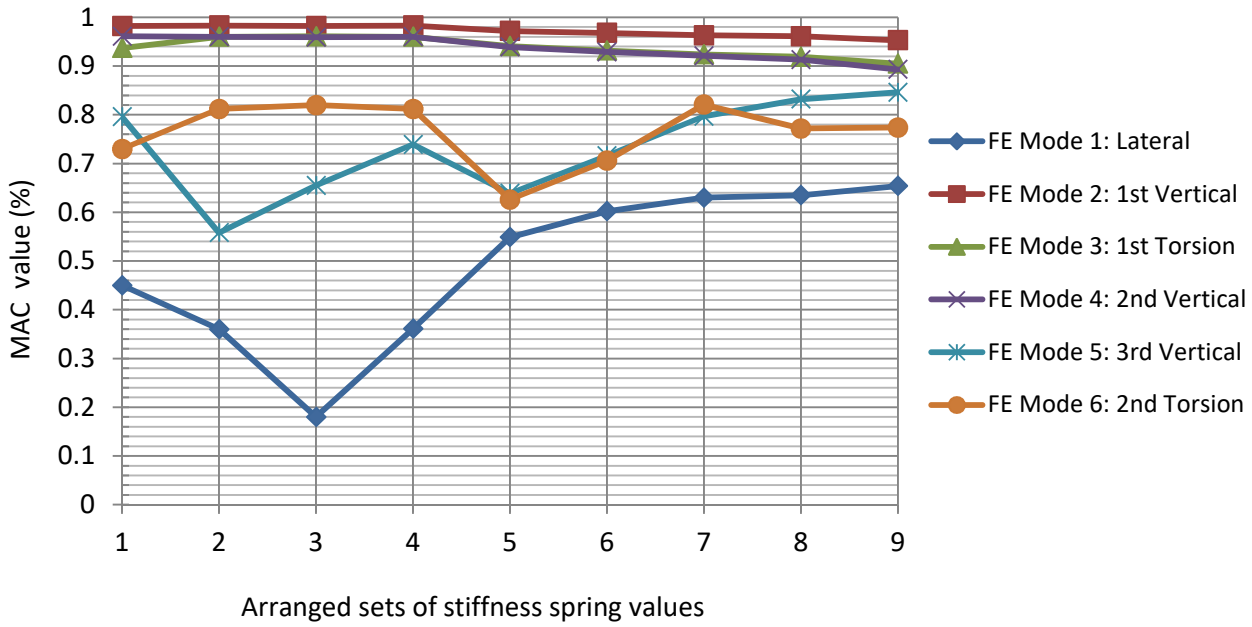

Figure 18: MAC calculated for arranged set of spring constants

As Table 2 represents (columns VII and IX), the frequency difference of all FE mode shapes was significantly reduced. The maximum frequency difference was for lateral mode shape; however, the value of frequency error has been reduced from 40.98% for initial model to 12.18% for updated model. For two modes of T2 and V3, the difference between FE-test frequencies was higher compared to the other three modes (V1, T1 and V2). Such a result could be anticipated as all the graphs for these two particular modes represented it clearly (Figures 12–17 given as two examples). However, the MAC values obtained from updating procedure were 85% and 77%, which indicated good agreement between FE-test mode shape counterparts. The largest difference in updating table was for lateral mode of 12.18%. The FE-test pair of this particular mode shape produced a MAC value of 65%. It is required to highlight that the lower frequencies resulted from other FE analyses could be selected for lateral mode, which led to lower frequency error, but their respective MAC values were lower than 65%. As the information in column V of Table 2 represented, the sequence of test mode shapes T2 and V3 was being reversed for their corresponding pairs of FE model.

Table 1: The values of starting and updated parameters

I - Parameter no.	II - Type	III - Location	IV - Starting value (N/m)	V - Updated parameter value (N/m)
1	Kx	P2	5.2E+7	6E+8
2	K_y	P2	10.1E+7	1.1E+9
3	K_z	P2	7.9E+6	9E+7
4	K_x	P3	4.9E+7	6E+8
5	K_y	P3	9.6E+7	1.1E+9
6	K_z	P3	8E+6	9E+7
7	K_x	P4	6.5E+7	7.5E+8
8	K_y	P4	9.3E+7	1E+9
9	K_z	P4	7.9E+6	9E+7
10	K_x	P5	5.2E+7	6E+8
11	K_y	P5	9.1E+7	1E+9
12	K_z	P5	8E+6	9E+7
13	K_x	P28	8.8E+7	1E+9
14	K_y	P28	1.03E+8	1.1E+9
15	K_z	P28	9.1E+6	1E+8
16	K_x	P38	8.8E+7	1E+9
17	K_y	P38	1.03E+7	1.1E+9
18	K_z	P38	9.6E+6	1.05E+8
19	K_x	P48	9E+7	1E+9
20	K_y	P48	1.04E+8	1.15E+9
21	K_z	P48	9.1E+6	1E+8
22	K_x	P58	8.7E+7	1E+9
23	K_y	P58	1.03E+8	1.1E+9
24	K_z	P58	9.6E+6	1.05E+8
25	K_x	P139	9.6E+7	1.05E+9
26	K_y	P139	1E+8	1.1E+9
27	K_z	P139	9.9E+6	1.1E+9
28	K_x	P159	9.6E+7	1.05E+9
29	K_y	P159	1E+8	1.1E+9
30	K_z	P159	9.9E+6	1.1E+9

Concerning the values obtained from manual updating procedure, a question could be raised: What level of agreement between measured and FE model properties is achievable? To find the answer, literatures dealing with dynamic assessment of bridges and footbridges through FE modelling and modal testing were reviewed. A brief presentation regarding the frequency errors of some previous works is as follows.

Table 2: Correlation between experimental and manually tuned FE model

I - Test mode no.	1	2	3	4	5	6
II - Ambient test $f(\mathrm{Hz})$	4.27	7.56	10.52	13.38	17.63	20.33
III - Mode description	Lateral	V1	T1	V2	T2	V3
IV - ξ (%)	10.21	2.52	1.27	4.92	2.13	3.89
V - FE mode no.	1	2	4	5	7	8
VI - Initial FEM $f(\mathrm{Hz})$	6.02	8.29	10.82	11.92	19.61	17.82
VII - Difference $\frac{(f_{VI} - f_{II})}{f_{II}}(\%)$	40.98	9.66	2.85	-10.91	11.23	-12.35
VIII - Updated FEM $f(\mathrm{Hz})$	4.79	7.41	10.44	13.16	18.75	18.34
IX - Difference $\frac{(f_{VIII} - f_{II})}{f_{II}}(\%)$	12.18	-1.98	-0.76	-1.64	6.35	-9.79
X - MAC (%)	65	95	90	89	85	77

The error in the natural frequencies for a suspension footbridge predicted by a reasonable FE model could be as large as 31.36% (Brownjohn et al. 1994). Turek et al. (2010) reported the frequency error value of 18.96% for an updated FE model of a bridge. The frequency difference value reported by Cantieni (2005) for an updated FE model of a bridge was 13.2%. The model of a pedestrian bridge validated by Galvin had a frequency error of 16.09% (Galvin and Dominguez, 2005). The frequency error of FE-test mode shapes for a timber footbridge reported by Diotallevi et al. (2008) was 11.45%. Ren and Zong (2004) identified the FE model of a bridge by maximum frequency error of 13.30%. The frequency difference of an FE model for a pedestrian bridge identified by Ndambi et al. (2005) was 23.16%. The reinforced concrete bridge that was modelled and investigated by Stewering and Fridhelm (2005) had an error frequency of 10.06%. Cantieni et al. (2008) updated the FE model of a filler beam bridge by maximum frequency difference of 12.85%. Zong et al. (2005) updated the FE model of an arch bridge by a maximum frequency difference of 11.08%. The error in natural frequency of an FE model updated by Hartley et al. (1999) was 11.8%. It should be stressed here that FE models of the case studies reviewed were

updated by using automatic updating software packages, which are specialised for updating and optimising purposes, whereas the method used for the current work is a manual updating method.

Figure 19 represents the FE-test mode shape counterparts for all six modes of vibration identified through AVT and updated by manual procedure. From the results given in Table 2 and Figure 19, it is concluded that the agreement of natural frequencies and mode shape pairs of manually updated FE model and test counterparts was good, and the total process of manual model updating for the footbridge in question was successful.

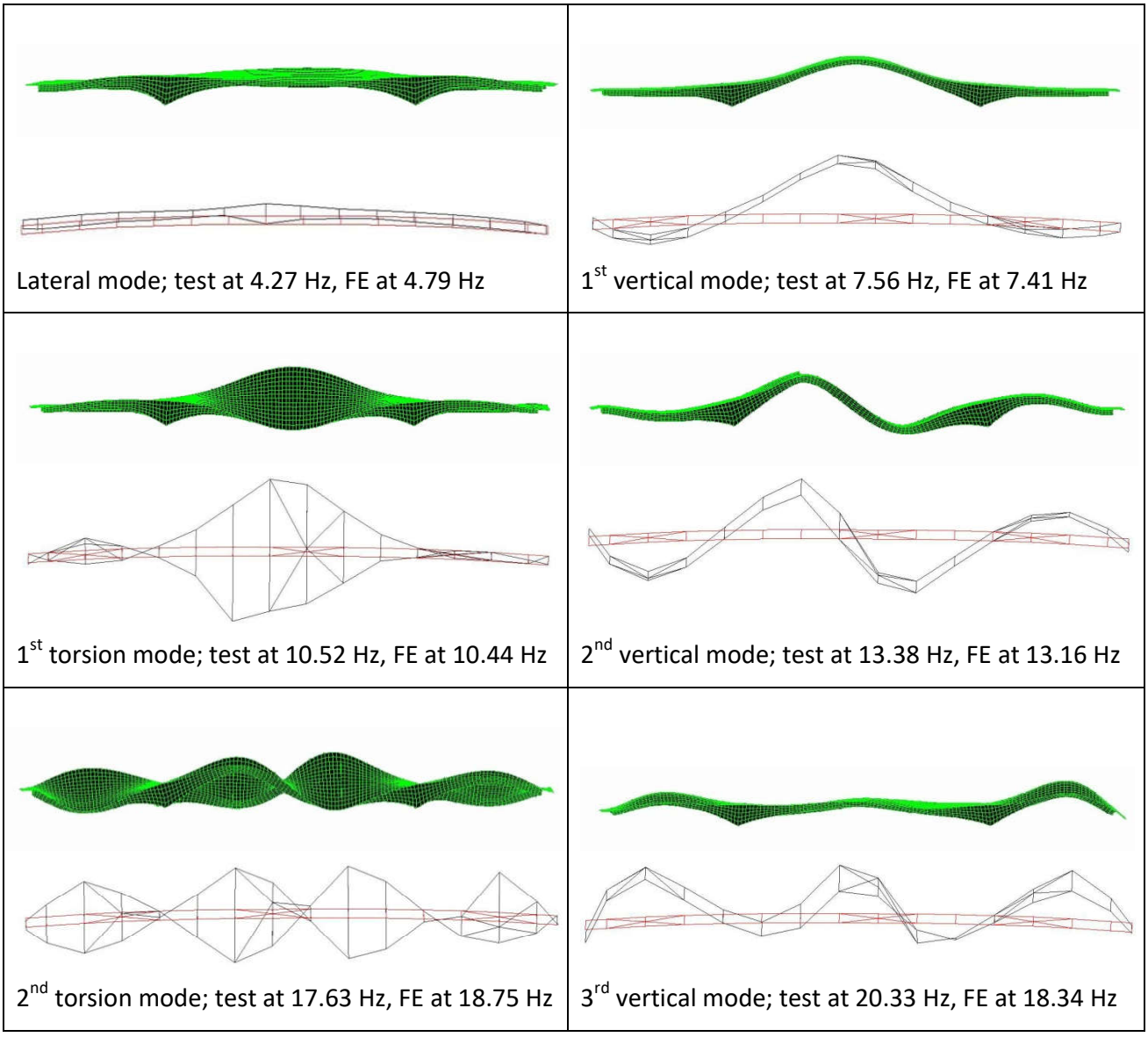

Figure 19. Display of mode shape pairs of updated FE and test models.

7. Conclusions

For updating purpose, a parametric study was performed on the most uncertain parameters of the FE model, which consist of boundary conditions, Young's modulus of elasticity (E) and mass density (r). The parametric study revealed that applying different E and r do not make considerable changes to the values of natural frequencies. It was found that the boundary conditions (stiffness values of spring sup-ports) were the most sensitive parameters that control the modal parameters for the case study. Therefore, 30 boundary conditions of the footbridge were selected as updating parameters. Computing the ratio of analytical to measured frequency for FE modes displayed the most appropriate range for manual model updating.

The target response selection was carried out based on three main criteria contributed to FE model updating, i.e. frequency, mode shape and MAC. Various sets of analytical mode shapes were calculated, and the values of frequencies were compared to their respective values of test mode shape counterparts. Subsequently, MAC was calculated using a modified formulation to quantify the comparison of vibration test and simulation results. The MAC values calculated from updated FE and test modes represented good agreement between all six modes of vibration. Applying updated parameter values of spring constants, the initial FE model was tuned and updated in a meaningful way so as to represent the best possible match with real condition of structure. The work highlights the importance of the form of optimization of the boundary conditions to achieve a precise FE model. Also, from the paper, the efficiency of manual updating procedure to estimate uncertain model parameters with high level of accuracy and obtain a more accurate numerical model is concluded.

References

Allemang, R.J., 1982. A correlation coefficient for modal vector analysis. In: IMAC I, USA.

Allemang, R.J., 2003. Modal assurance criterion – twenty years of use and abuse. Journal of Sound and Vibration, 37, 14–23.

ARTeMIS, 1999–2002. ARTEMIS Extractor Pro. Aalborg, Denmark: Structural Vibration Solutions.

Avitabile, P., 1998. Overview of analytical and experimental modal model correlation techniques. Modal analysis and controls laboratory, University of Massachusetts Lowell.

Brownjohn, J.M.W., Dumanoglu, A.A., and Taylor, C.A., 1994. Dynamic investigation of a suspension footbridge. Engineering Structures, 16, 395–406.

Brownjohn, J.M.W., et al., 2010. Ambient vibration re-testing and operational modal analysis of the Humber Bridge. Engineering Structures, 32, 15.

Caetano, E. and Cunha, A., 2004. Experimental and numerical assessment of the dynamic behaviour of a stress-ribbon bridge. Structural Concrete, Journal of FIB, 5, 10.

Cantieni, R., 2005. Experimental methods used in system identification of civil engineering structures. In: 1st IOMAC, Copenhagen, Denmark.

Cantieni, R., et al., 2008. Ambient testing and model updating of a filler beam bridge for high-speed trains. In: 7th EURODYN, Southampton, UK.

Cunha, A. and Caetano, E., 2006. Experimental modal analysis of civil engineering structures. Sound and Vibration, 40, 12–20.

DIANA, 2009. DIANA finite element analysis. Delft, Netherlands: TNO DIANA BV.

Diotallevi, P.P., Manfroni, O., and Belmonte, C., 2008. Forced vibration tests carried out on a laminated timber footbridge: comparisons five years apart. In: 3rd Inter-national Footbridge Conference, Porto, Portugal, University of Porto.

Ewins, D.J., 1997. Model validation: correlation for updating. SADHANA, Bangalore, 25, 221–234.

Galvin, P. and Dominguez, J., 2005. Modal identification of a pedestrian bridge by output-only analysis. In: SEM: IMAC XXIII, USA.

Hartley, M.J., Pavic, A., and Waldron, P., 1999. Investigation of pedestrian walking loads on a cable stayed footbridge using modal testing and FE model updating. In: IMAC XVII, USA.

Maia, N.M.M. and Silva, J.M.M.E., 1997. Theoretical and experimental modal analysis. Somerset, England: Research Studies Press LTD.

Ndambi, J.-M., Giannopoulos, G., and Vantomme, J., 2005. Dynamic characterisation of an IPC pedestrian bridge. Engineering Structures, 27, 229–237.

Pavic, A., Hartely, M.J., and Waldron, P., 1998. Updating of the analytical models of two footbridges based on modal testing of full-scale structures. In: ISMA 23, Leuven, Belgium.

Ren, W.-X. and Zong, Z.-H., 2004. Output-only modal parameter identification of civil engineering structures. Structural Engineering and Mechanics, 17, 1–16.

Reynders, E., et al., 2010. Combined experimental operational modal testing of footbridges. Journal of engineering mechanics (ASCE), 136, 687–696.

Stewering, U. and Fridhelm, S., 2005. Finite element modelling of a reinforced concrete bridge and comparison with vibration measurement. In: SAMCO, Zell am See, Austria.

Turek, M., Ventura, C., and Dascotte, E., 2010. Model updating of the ironworkers memorial second narrows bridge, Vancouver, Canada. In: IMAC XXXI, Jacksonville, Florida.

Zong, Z.-H., et al., 2005. Dynamic analysis of a half-through concrete-filled steel tubular arch bridge. Engineering Structures, 27, 3–15.